

APPROVAL SHEET

Title of Thesis: Wireless bipotentiostat circuit for glucose and H₂O₂ interrogation.

Name of Candidate: Priyanka
Annamalai,
Master of Science,
2019

Thesis and

Abstract

Approved:

Dr. Gymama Slaughter
Assistant Professor of Computer Engineering
Department of Computer Science and Electrical Engineering
University of Maryland, Baltimore County.

Date Approved:

ABSTRACT

Title of Thesis: Wireless bipotentiostat circuit for glucose and H₂O₂ interrogation

Priyanka Annamalai, MS, 2019

Thesis directed by: Dr. Gymama Slaughter,
Director for Bioelectronics Laboratory
Department of Computer Science and
Electrical Engineering

Here we present a cost-effective point-of-use wireless platform for the electrochemical detection of low concentrations of glucose and hydrogen peroxide (H₂O₂) simultaneously. The electrochemical system utilizes a dual sensor integrated with a portable bipotentiostat. The bipotentiostat hardware implements a basic design that reduces the cost of construction and increases the affordability of the instrument, while providing similar functionality to the more expensive bench-top potentiostats. The bipotentiostat utilizes inexpensive components, common Ag/AgCl reference and platinum counter electrodes, two working electrodes, and it is designed to detect currents within the range of 20 uA to 7 mA. Additionally, the bipotentiostat is integrated with wireless module ESP8266 that interfaces with a smartphone to enable real-time monitoring and visualization of the analyte concentration levels. The results show that the self-designed bipotentiostat is capable of performing chronoamperometry and demonstrate an electrochemical detection system that is a portable alternative system for laboratory and point-of-use testing.

Wireless bipotentiostat circuit for glucose and H₂O₂ interrogation

By

Priyanka Annamalai

Thesis submitted to the Faculty of the Graduate School of the University of Maryland in partial

fulfillment

of the requirements for the degree of

Master of Science

2019

Dedicated to my parents Santhi Annamalai and P. Annamalai, my brother Aswath Kirthik and all my friends and family.

Acknowledgements

Firstly, I would like to express my sincere gratitude to my advisor Professor Gymama Slaughter for the continuous support for my research work and her patience, motivation and immense knowledge. Her guidance has helped me in all times of research and writing of this Thesis. I also thank my committee members Dr. Nagmeh Karimi and Dr. Jiaqi Gong for their encouragement and insightful comments. My sincere thanks to Dr. J. Shankara Narayanan for helping and supporting me with the research work. I thank my fellow lab mates Ankit Baingane, Md Hasan Qumrul, Ressa Sarreal, Saikat Banerjee and Adam Der for their support.

Last but not the least, I would like to thank my family, my parents and brother for supporting me throughout my journey.

Table of Contents

LIST OF FIGURES.....	v
Chapter I: Introduction.....	1
A. Motivation.....	1
B. Thesis Statement	3
C. Author's Contribution.....	4
D. Thesis Outline	5
Chapter II: Background.....	6
A. Electro-Analytical Methods of Analysis	16
B. Bipotentiostat.....	19
Chapter III: Wireless Biosensor	23
A. ESP8266.....	27
Chapter IV: Construction of wireless bipotentiostat circuit for analyte interrogation ..	33
A. Materials	36
B. Electrode Construction.....	36
Chapter V: Experimental Results	38
Chapter VI: Conclusion	46
A. Future Work	46
References	47

LIST OF FIGURES

Figure 1: Model-based county-level estimates of the age-adjusted prevalence of diagnosed diabetes	1
Figure 2: Total number of mobile phone users worldwide from 2015 to 2020	2
Figure 3: Wireless Bipotentiostat block diagram.....	5
Figure 4: Eyeglass Biosensor System	212
Figure 5: Conceptual diagram of an active contact-lens system for wireless health.....	24
Figure 6: Glucose-sensing tattoo printed onto a tooth platform	25
Figure 7: Electrochemical Cell	26
Figure 8: Two-Electrode Configuration.....	17
Figure 9: Three-Electrode Configuration.....	17

Figure 10: Schematic of Potentiostat Circuit	18
Figure 11: Potentiometric Titration	190
Figure 12: A plot showing relation between current and time provided by coulometry	31
Figure 13: Voltammetry.....	32
Figure 14: The voltage causes changes in current waveform - Chronoamperometry	32
Figure 15: Schematic of Bipotentiostat.....	33
Figure 16: Multielectrode GCE Potentiostat.....	34
Figure 17: Multielectrode Amperometric Biosensor	34
Figure 18: Parallel Architecture using Array of Working Electrodes	35
Figure 19: Commercial Potentiostat	36
Figure 20: The Comparison between various wireless standards	37
Figure 21: Network Architecture of CAN	39

Figure 22: UWB Transmitter	40
Figure 23: UWB Receiver	40
Figure 24: Measuring System	41
Figure 25: ESP8266	42
Figure 26: NodeMCU	44
Figure 27: Pinout Diagram for NodeMCU	44
Figure 28: Adafruit Website	46
Figure 29: MQTT Mobile Application	47
Figure 30: Wireless Bipotentiostat Block Diagram	49
Figure 31: Schematic of Bipotentiostat.....	50
Figure 32: Glucose calibration plot measured using constructed bipotentiostat(100 mM PBS, ph 7.4).	54

Figure 33: H ₂ O ₂ calibration plot measured using constructed bipotentiostat(100mM PBS, ph 7.4).	54
Figure 34: Selectivity behavior of the glucose sensor measured in the presence of interference series	54
Figure 35: Selectivity behavior of the H ₂ O ₂ sensor measured in the presence of interference series	57
Figure 36: Experimental Setup	59
Figure 37: Adafruit website displaying the concentration of glucose	60
Figure 38: MQTT Application showing glucose concentration	61

Chapter I: Introduction

A. Motivation

The number of people worldwide with diabetes has risen from 108 million in 1980 to 422 million in 2014 [1]. In the United States, an estimated 30.3 million people of all ages, or 9.4% of the country's population, had diabetes in 2015[2] as shown in Figure 1 below:

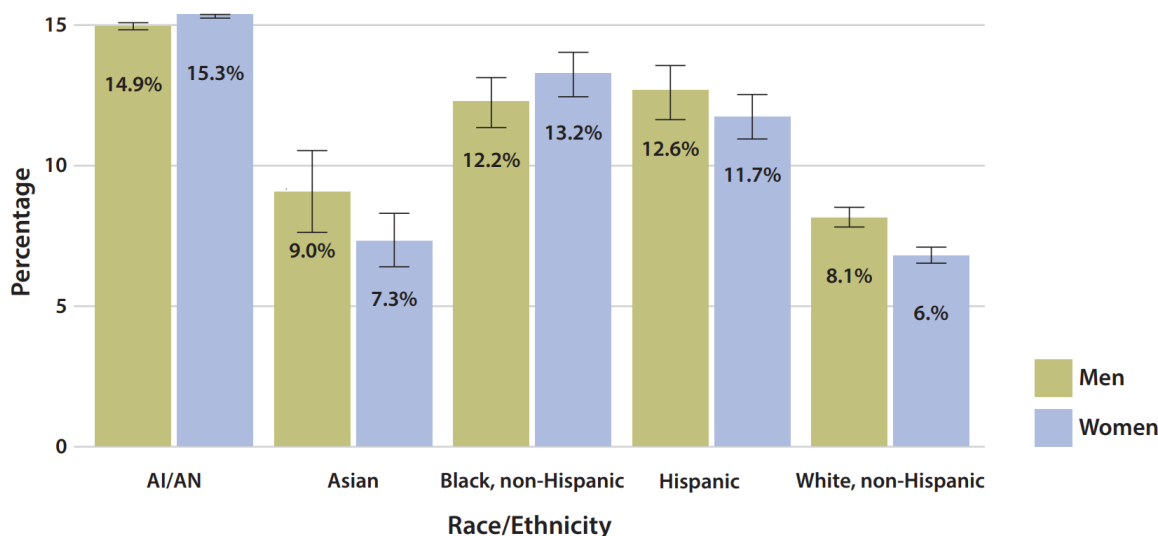


Figure 1: Model-based county-level estimates of the age-adjusted prevalence of diagnosed diabetes. Adapted from Diabetes Online [2]

Meanwhile, hydrogen peroxide (H_2O_2) is a reactive oxygen species which can respond to various cellular targets' functions as a signaling molecule that controls different essential processes in mammals and plants. Excess H_2O_2 is implicated in arteriosclerosis, organ failure, cancer, stroke, diabetes, and a host of other serious diseases [3]. Therefore, real-time detection of glucose and H_2O_2 plays an important role in the diagnosis and treatment of diseases.

Recently, miniaturized portable potentiostats have been constructed for the electrochemical detection of such biochemical analytes. However, the cost of fabrication, complicated

construction procedure, and circuit designs of the commercial potentiostats are inaccessible to those who need an affordable potentiostat for medical diagnostics and wearable devices for personal health monitoring. The importance of simple, low-cost, portable, electrochemical detectors for point-of-care diagnostics are well recognized and are extensively studied [4-8]. Most of these electrochemical detectors are designed to work with a wired computer using a USB port and does not offer connection to mobile devices [6]. Additionally, more than 50% of the world's population that owns mobile devices also own a smartphone with advanced computing capabilities and connectivity as shown in Figure 2 [9] below:

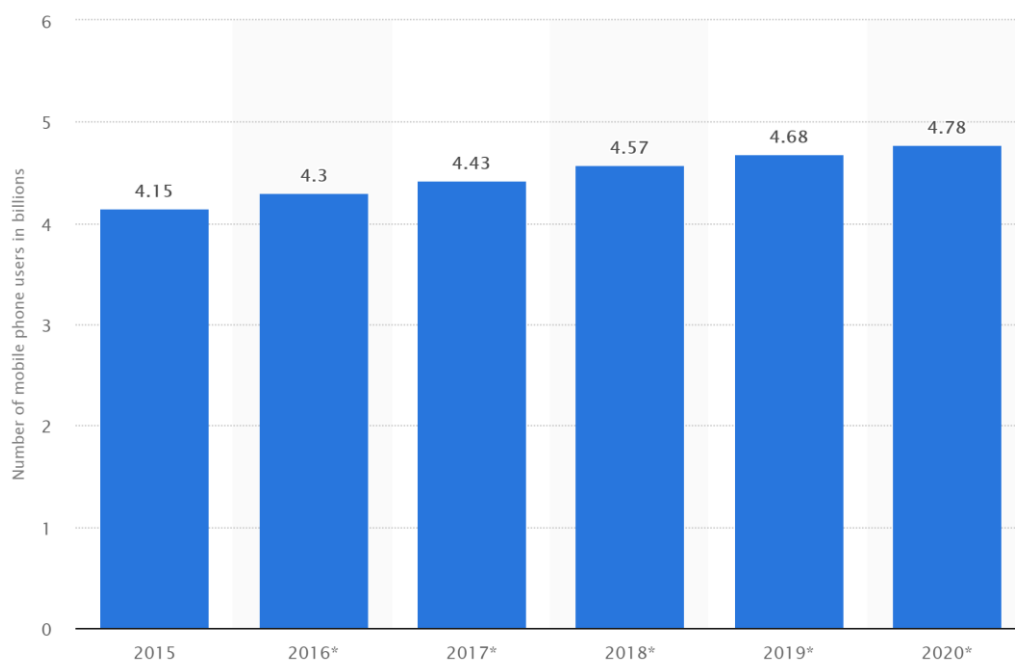


Figure 2: Total number of mobile phone users worldwide from 2015 to 2020. Adapted from statista.com [9]

A portable potentiostat with wireless connectivity to smartphones would enable facile point-of-use and in-the-field analysis of metabolites, where access to a computer may not be possible. Among various analytical techniques used in commercial sensors, electrochemical sensors are very attractive because of their reliability, stability, long-term use, and good

selectivity [10]. To improve potentiostat sensitivity, the electrochemical transduction elements are constructed with different materials such as electrodeposition of metal oxides [11,12], CNTs [13–15], zinc-decorated graphene oxide [16], ionic liquid film dipping method [17], self-assembly [18–20], and co-polymerization of a conducting polymer [21,22]. Although these modifications have advantages to enhance the sensitivity of the sensors, they suffer from poor selectivity and biocompatibility. Therefore, noble metals are widely used to address these challenges [23,24]. The unique properties of noble metal nanoparticles, such as low toxicity and high surface area, make them attractive for the construction of electrochemical sensors with enhanced analytical performance.

Based on the prior work on development of wireless and connected electrochemical detectors for a specific application, very little attention has been focused on the development of a wireless bipotentiostat for monitoring two analytes simultaneously. Here, we describe the design and characterization of a low cost portable wireless electrochemical detector for the sensitive and selective determination of glucose and H_2O_2 . The fabricated sensor is integrated with the wireless electrochemical detector system that can be powered by a battery. This electrochemical system is capable of monitoring two analytes of interest in real-time via a mobile device. The glucose and H_2O_2 sensors are fabricated using colloidal platinum electrodeposited on gold microwire and tungsten microwire decorated with AuNP and horse radish peroxidase (HRP), respectively to realize dual sensing of glucose and H_2O_2 .

B. Thesis Statement

The thesis focuses on the development of a wireless bipotentiostat circuit that can

monitor the concentrations of both glucose and hydrogen peroxide, which are very essential biomarkers of health. The biosensor can be used to monitor the particular analyte concentration levels in the target sample (i.e., tissue, organ, blood, etc).

C. Author's Contribution

Here a final version of the bipotentiostat was designed and fabricated for testing with glucose and H_2O_2 solutions. The Bipotentiostat circuit uses operational amplifiers that are commonly available, and at a lower price point. Additionally, not many electrochemical detectors have been developed to measure the concentration of two analytes simultaneously. The electrodes needed to be carefully constructed with the necessary biorecognition element such as enzymes in order to be used in experiments testing for various analytes in solution. The current generated in the presence of glucose solution is a result of oxidation of the analyte while a current generated in the presence of H_2O_2 is due to reduction of the analyte. Hence, the operations taking place required reduction-oxidation (redox) reactions. Hence, designing the circuit accordingly was a challenge. The oxidation of glucose should not be affecting the reduction of the H_2O_2 . Thus, inverters were employed in the circuit design. The biopotentiostat was then wirelessly integrated using microcontrollers to interface with a personal computer and synced with a mobile device. The use of microcontrollers and other interfaces added to the circuit complexity. The NodeMCU wireless module was small in size and had a built-in microcontroller which enabled data processing and wireless transmission onto the real-time dashboard which can be synced with the mobile device through an android application. The block diagram of the system is given as shown in Figure 3.

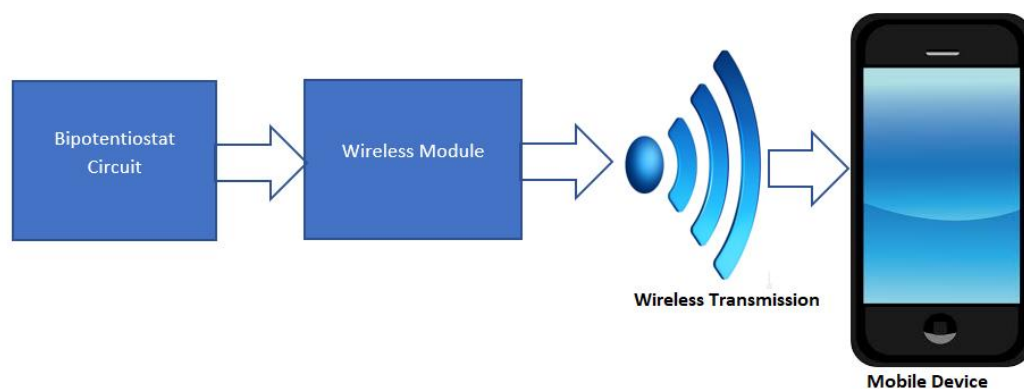


Figure 3: Wireless bipotentiostat block diagram.

D. Thesis Outline

The purpose of Chapter 2 is to provide background to the thesis and introduce the reader to the working principle of the potentiostat circuit, bipotentiostat circuit, and the different approaches that have been used previously. Chapter 3 introduces the concept of wireless integration. The details regarding the hardware and software implementations are explained. Chapter 4 discuss the experimental set up, data and results obtained. Chapter 5 provides a conclusion on the work performed and the future work.

Chapter II: Background

A non-invasive and continuous wearable glucose-sweat sensing device has been reported [25]. Sensors integrated in to this Bluetooth-enabled wristband detect skin temperature, sodium, potassium, lactate, and glucose concentrations in sweat. An advantage of this approach is the use of multiple sensors which overcomes the limitations of single, stand-alone sensors. Due to the complex nature of sweat, multiple sensors are required to provide a more comprehensive profile of sweat composition and enable data cross-comparisons. For example, it is known that the potassium concentration in sweat is quite stable during basal and exercising states. As a result, potassium levels can be used as a reference for comparing the fluctuating concentrations of other analytes, such as glucose, and enable real fluctuations to be distinguished from artefacts. This device was designed to exhibit similar form factors of existing devices, such as the fitness wristbands by Fitbit Inc. (San Francisco, CA, USA), thereby encouraging user uptake to create a pathway to commercialization [26]. The sensors were tested individually in situ and collectively in the device. The device analyte readings showed a correlation to the normal concentration ranges in sweat during exercise and the sensors could be used for continuous operation for up to two hours before the glucose and lactate sensing units were interchanged for fresh sensor arrays. A minimum of 10 μ L of sweat was required before any sweat analysis could be achieved. The sensors were placed close to the skin, to allow for immediate analysis of sweat as it emerged. Sweat was absorbed into a water-absorbent thin rayon pad for stable and reliable glucose readings, placed between the electrode sensors and skin. This flexible wearable sensing system is a promising platform for

tracking multiple physiological analytes during exercise. The Wearable Sweat Sensor system is as shown in Figure 4 [26].

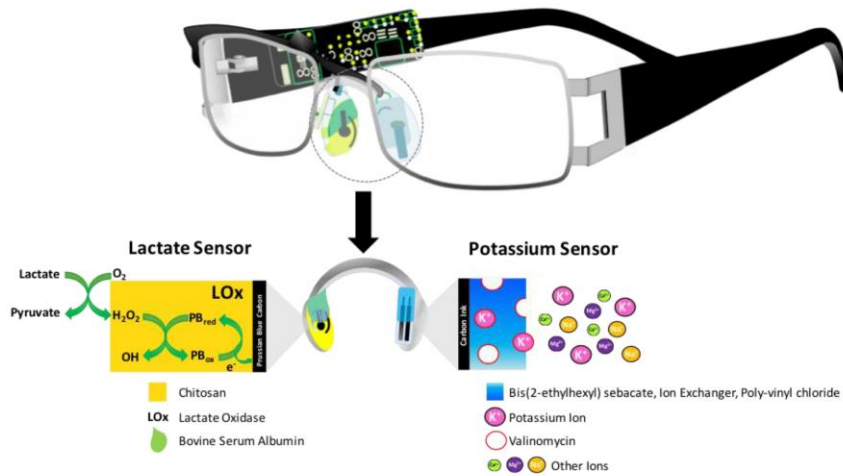


Figure 4: Eyeglass Biosensor System. Adapted from D. Bruen.et.al [26]

Liao et al. developed a tear glucose monitoring sensor system that integrates a loop antenna, wireless sensor interface chip, and glucose sensor on a polymer substrate [26]. The IC consists of power management, readout circuitry, wireless communication interface, LED driver, and energy storage capacitors in a 0.36-mm CMOS chip with no external components. The sensitivity of the glucose sensor was reported to be $0.18 \mu\text{A mm}^{-2} \text{mM}^{-1}$. The system is wirelessly powered and achieves a measured glucose range of up to 0.051 mM with a sensitivity of 400 Hz/mM while consuming 3 W from a regulated 1.2-V supplies. The on-lens electrochemical sensor provides real-time continuous glucose monitoring and high sensitivity compared to conventional glucose monitoring. The sensor directly accesses the tear fluid and thus can improve the sensitivity and reduce the sampling processes and potential of infection during operation.

There are many challenges in the implementation of the on-lens sensor system. First, the system is extremely constrained by power and area. A standard contact lens has an area of about 1 cm and a total thickness of about 200 μ m. Component size in the design is severely restricted, roughly 1 mm, which is determined by the curvature of the eye and the assembly process. Clearly, standard surface-mount components are too large for integration onto a contact lens. In addition, volume limitations remove the possibility of large energy storage devices. Therefore, a biosensor on a contact lens must be powered wirelessly through external sources (e.g., RF power, inductive power, or optical power) [26].

Third, the active contact lens system requires the heterogeneous biocompatible integration of different devices/materials on a plastic substrate. Possible issues of using the sensors on the eye may include RF-power caused eye temperature increase, vision-blocking, and damage from on-lens device. The regulation of RF-power-caused temperature shifts still under study for human eyes. The process has adhered to the IEEE C95 standard to minimize risk in this area. To reduce the intrusion of and damage to the equipment, on-lens devices can be embedded into the lens. The devices on the contact lens are out of the focus of human eyes and are placed outside the lens to further avoid vision blurring. Also, Google Contact Lens are being developed by the collaboration of Novartis and Google with a planned introduction by 2020. The lens is proposed to contain a tiny and ultra slim microchip that is embedded in one of its thin concave sides. Through it's a tiny antenna, it will send data about the glucose measurements from the users tears to his or her paired smartphone via installed software. Initially, developers were also considering adding LED lighting that could help warn users when their glucose levels dropped below certain thresholds. However, they abandoned the idea, as the arsenic composition of the LED could prove dangerous.

If successful, the lens would offer an easier and more comprehensive way of monitoring the glucose levels of diabetics compared to the current techniques, which include drawing blood from the finger of the patient. The technology has the potential to lower the cost of managing chronic diseases and to encourage people become involved in managing their health digitally. A statistical investigation earlier last year revealed that the contact lens has been dismissed by many researchers and even by the experts inside Novartis and Google as technically infeasible because tears have proved not as reliable in measuring glucose levels in humans compared to extracting blood. An expert in non-invasive glucose technologies, former Chief Security Officer (CSO) of Johnson & Johnson(J&J)'s company - LifeScan, John Smith mentioned that efforts to measure blood sugar through saliva, sweat, and tears have failed for decades [26]. He called the diabetes-assistive contacts lens, faith-based science; further, he says it cannot produce glucose readings and is prone to be impacted by external variables such as the surrounding environment, temperature, and humidity. Competitors are now taking advantage of Novartis and Google contact lens issues to work on their own smart eye wearables. EPGLMed, for example, is working with Google's rival, Apple, to develop its own lens [27]. The Conceptual diagram of the Tear-Glucose monitoring system is as shown in Figure 5 below.

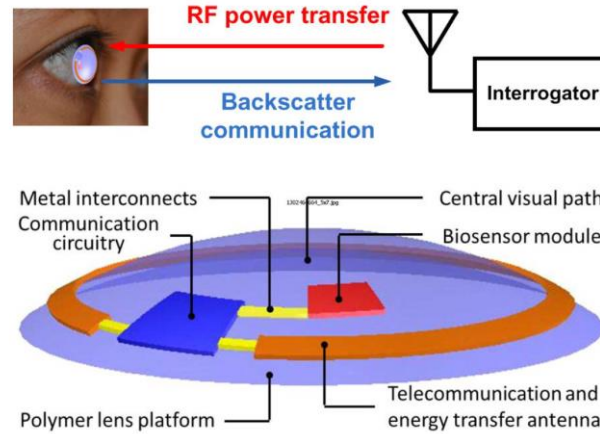


Figure 5: Conceptual diagram of an active contact-lens system for wireless health. Adapted from Yu-Te Liao, et.al [27]

Intraoral dental accessories have also been of interest for non-invasive and continuous monitoring to provide information regarding a patient's health status. A tooth has the potential to act as a continuous monitoring device as it is in constant contact with the patient's saliva. Mannoor et. al have developed a bacterial detection approach whereby a graphene-based nanosensor was printed on to a water-soluble silk and transferred onto tooth enamel [26]. This sensing tooth incorporates a resonant coil to prevent the need for a power source and external connections. The device operates by self-assembling antimicrobial peptides on to the single sheet of graphene, where the bio-selective analysis of bacteria can be performed at a single cellular level. Preliminary results showed great specificity, response time, and single-molecule detection abilities for this sensor, however this sensing application must still be tested on-body for real-time analysis. This approach could potentially be adapted for detection of other analytes such as glucose, by means of a chemical glucose sensor immobilized on to a water-soluble silk layer attached to the tooth enamel [26]. The Glucose sensing tattoo is shown in Figure 6.

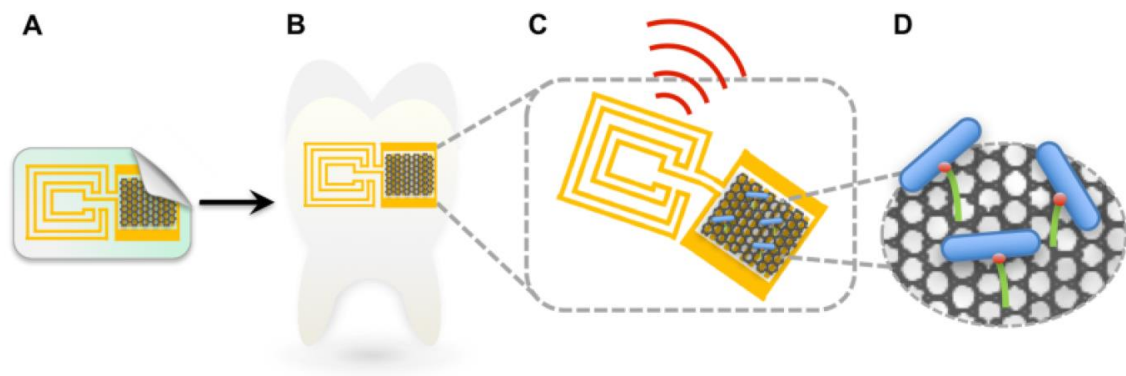


Figure 6: Glucose-sensing tattoo printed on to a tooth platform as a non-invasive continuous. Adapted from D. Bruen.et.al [26]

Mainly all the sensors discussed so far are glucose sensors, which have three electrodes – the working Electrode (WE), the counter Electrode (CE), and the reference Electrode (RE) wherein the working Electrode is coated with glucose sensitive enzyme in order to form the glucose sensor. These electrodes dipped in a liquid containing glucose (sweat, saliva, blood, tears) form an electrochemical cell. This enables the sensors to detect the level of glucose present in the respective liquid.

Electrochemical Cell

An electrochemical cell is a device capable of either generating electrical energy from chemical reactions or using electrical energy to cause chemical reactions. An example of an electrochemical cell is shown in Figure 7. Here, there are two metal electrodes which are dipped into electrolyte where a chemical reaction either uses or generates an electric current. The two electrodes are connected through the salt bridge carrying ions between them.

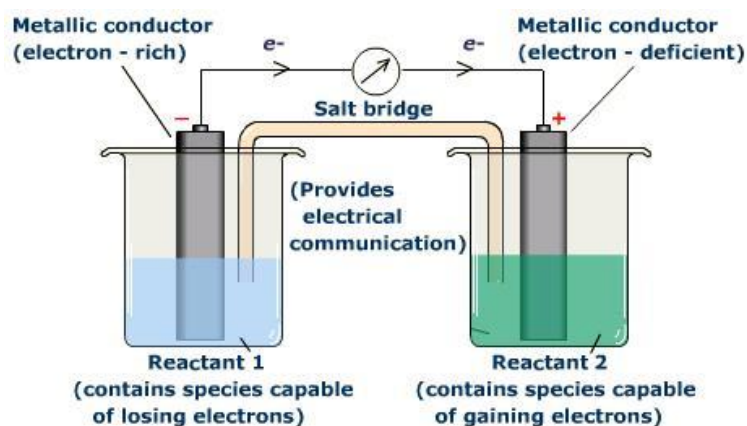


Figure 7: Electrochemical Cell. Adapted from Wikipedia.

There are two main electrode configurations: The two-electrode configuration and the three-electrode configuration [28]. The two-electrode configuration consists of two electrodes – the working electrode and the auxiliary/counter electrode. The applied potential is measured between the working and the counter electrodes and the resulting output current is measured in the working or counter lead. The counter electrode plays a dual role, wherein 1) it completes the circuit for the current to flow through the electrochemical cell and 2) it maintains a constant voltage in the cell irrespective of the current flowing through the cell. Under the two-electrode configuration it is difficult for the counter electrode to play a dual role and that is the disadvantage of this configuration. This is further exacerbated by the need to maintain constant counter electrode potential when the current is flowing through the working electrode and counter electrode. The two-electrode configuration is depicted in Figure 8. The three-electrode configuration addresses this challenge. The three electrode configuration consists of a working electrode, reference electrode, and the counter

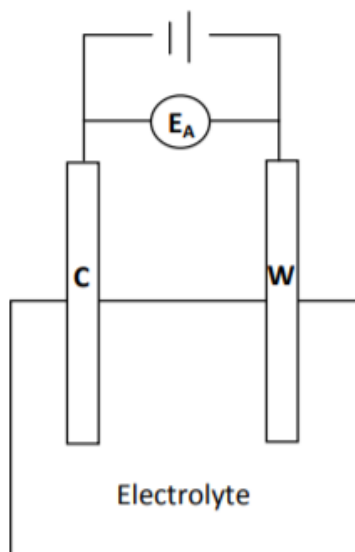


Figure 8: Two-Electrode Configuration. Adapted from Prashant Kamath [28]

electrode. The reference electrode acts as a reference in measuring and controlling the working electrode potential. The reference electrode passes a very negligible current and hence the voltage drop between the reference electrode and the working electrode is very small. Thus, the reference potential is much more stable in a three-electrode system. The most common reference electrodes used are the saturated calomel electrode and the Silver/ Silver Chloride (Ag/AgCl) electrode.

Here the role of the counter electrode is to complete the circuit and pass all the current needed to balance the current observed at the working electrode. The counter electrode isolates this reference electrode and passes all the current through it. The working electrode is the electrode where the potential is measured, and current is flowing as depicted in Figure 9.

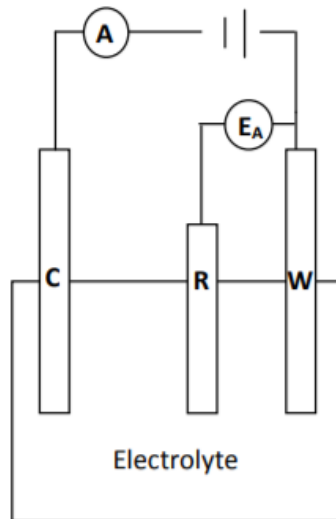


Figure 9: Three-Electrode Configuration. Adapted from Prashant Kamath [28]

The purpose of a potentiostat is to control the voltage between the working electrode and the reference electrodes. Both electrodes are contained in the electrochemical cell. The potentiostat implements this control by injecting a current into the cell through the auxiliary electrode/counter electrode. The potentiostat typically contains four main parts [29]: the electrometer, I/E converter, control amplifier, and the signal circuit. The schematic of the Potentiostat circuit is as shown in Figure 10. The electrometer circuit measures the voltage difference between the working and the reference electrode. Its output serves two purposes: it acts as a feedback signal within the potentiostat, and it is the voltage signal that is measured and displayed to the user. An ideal electrometer has infinite impedance and zero current. In reality, the reference electrode does pass a very small amount of current. Current through the reference electrode can change its potential, but this current is usually so close to zero that the change is negligible. The capacitance of the electrometer and the resistance of the reference

electrode form an RC-filter. If the RC time constant is too large it can limit the effective bandwidth of the electrometer. The electrometer bandwidth must be higher than the bandwidth of all other components in the potentiostat.

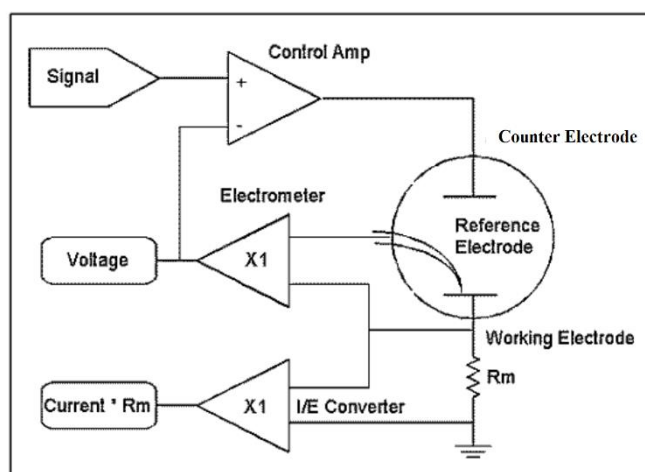


Figure 10: Schematic of Potentiostat Circuit. Adapted from gamry.com [29]

The I/E converter (current to voltage converter) is used to measure the cell current. The cell current is forced through a current measurement resistor, R_m . The resulting voltage across this resistor is a measure of cell current. X1 in Figure 7 on an amplifier indicates it's a unity gain amplifier. During the course of an experiment, cell current can change by several orders of magnitude. Such a wide range of current cannot be accurately measured by a single resistor. Modern potentiostats have a number of R_m resistors and an "I/E autoranging" algorithm that selects the appropriate resistor and switches it into the I/E circuit under software control. The bandwidth of the I/E converter depends strongly on its sensitivity. Unwanted capacitance in the I/E converter along with R_m , forms an RC circuit. In order to measure small currents, R_m must be sufficiently large. This larger resistance, however, increases the circuit

limit RC time constant on the I/E bandwidth.

The control amplifier compares the measured cell voltage to the desired cell voltage and drives current into the cell to force these voltages to be the same. The control amplifier works on the principle of negative feedback. The measured voltage enters the amplifier in the negative or inverting input. Therefore, a positive perturbation in the measured voltage creates a decrease in the control amplifier output, which counteracts the initial change. The control amplifier has a limited output capability, for example, in the case of the Gamry Instruments' Reference 3000, the control amplifier cannot output more than 32 V, or more than 3 A. Proper choice of number sequences allows the computer to generate constant voltages, voltage ramps, and sine waves at the signal current output.

A. Electro-Analytical Methods of Analysis

Electrochemical reactions involve an exchange of electrons between reactants and products. Such a process can be induced by application of electrical energy to electrodes placed in electrically conducting solutions. Electro-analytical techniques involve measurement of potential difference, current, or conductance of solutions. There are four main electro-analytical techniques: potentiometry, Coulometry, voltammetry and chronoamperometry.

Potentiometry involves measurement of potential difference across the working and reference electrodes immersed in a solution. In case of potentiometric titration, the potential difference is plotted against volume of reagent added and equivalence point read from the plot as depicted in Figure 11 [30].

Potentiometric titration

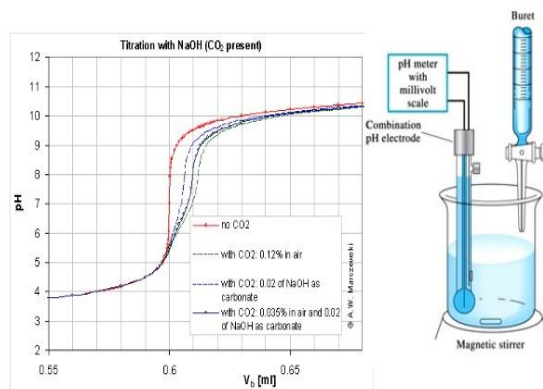


Figure 11: Potentiometric Titration. Adapted from Wikipedia [30]

In coulometry, electrolysis is carried out until the analyte is completely oxidized or reduced to the final product. Here, the current is measured in terms of total number of electrons generated [31]. This is depicted in Figure 12.

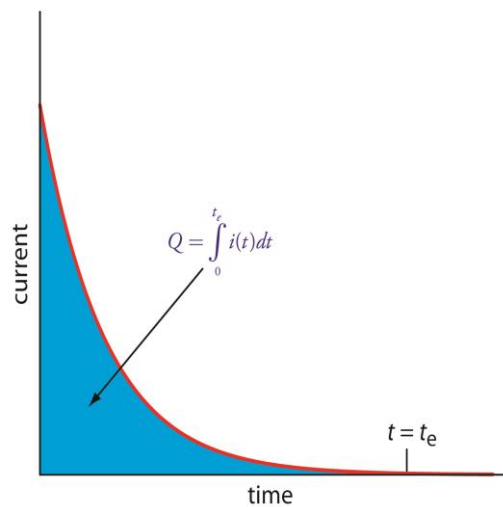


Figure 12: A plot showing the relation between current and time provided by Coulometry. Adapted from Wikipedia [31]

Voltammetry involves changes in concentration of the electroactive entity through oxidation

or reduction at the surface layer at the working electrode such as gold, platinum, glassy carbon, or mercury. The resulting current is plotted as a function of applied potential as illustrated in Figure 13 [31].

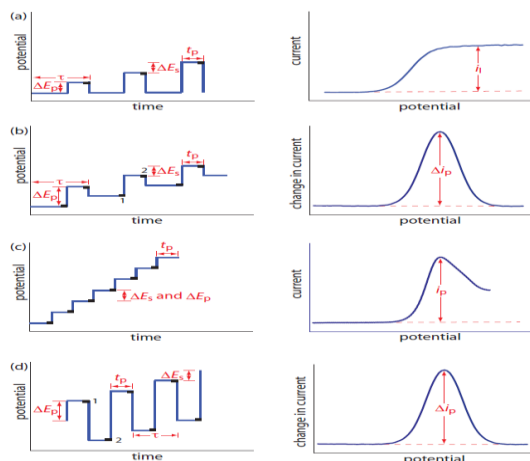


Figure 13: Voltammetry. Adapted from Wikipedia [31]

Chronoamperometry involves the measurement of the current between two electrodes at constant potential difference. The current is plotted against the concentration of the analyte. This is a time-dependent technique where the voltage is applied to the working electrode and resulting current is measured as a function of time [31].

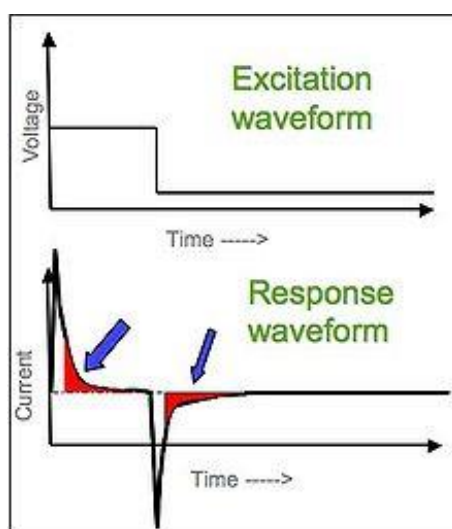


Figure 14: The voltage causes changes in current waveform in case of Chronoamperometry. Adapted from Wikipedia [31]

The chronoamperometry technique is used in this work to measure the current values and apply a constant voltage between the reference and working electrodes.

B. Bipotentiostat

Bipotentiostat is used for dual sensing of the analyte based on the current flowing through the respective electrodes. This system uses two working electrodes to sense the concentration of the analytes based on current flowing through each electrode, respectively. Figure. 15 shows the schematic of Bipotentiostat:

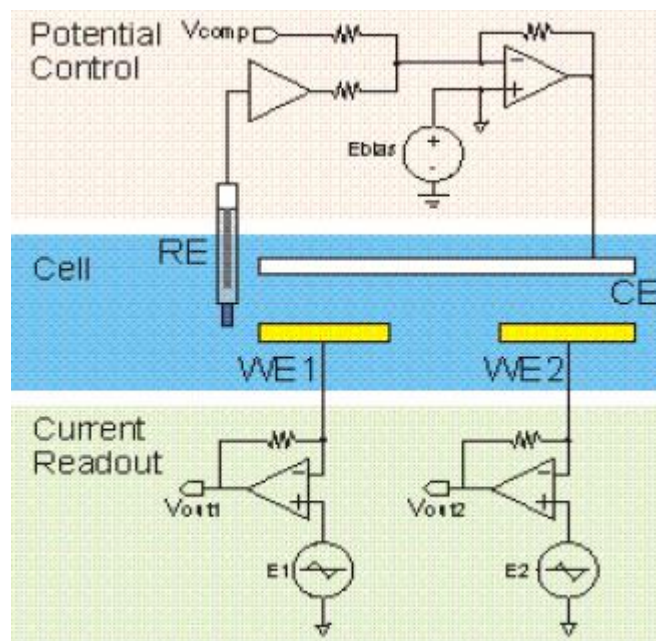


Figure 15: Schematic of Bipotentiostat. Adapted from Y. Huang, Et. al [32]

The grounded counter electrode method uses two working electrodes and two reference electrodes placed close to each other and the counter electrode is grounded. Thus, this ensures the currents flowing through the two solutions do not affect each other. When the two solutions contain only one species, and the other is water, the current is reduced [33]. The grounded

counter electrode is as shown in Figure 16.

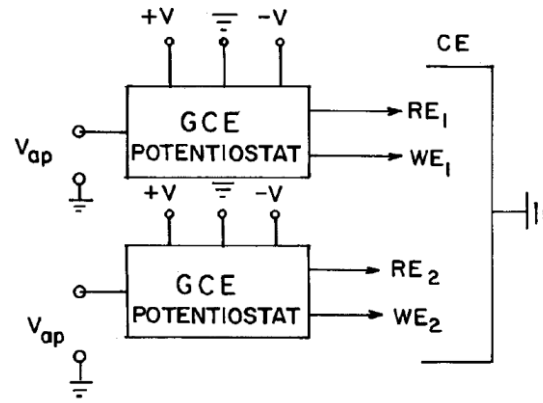


Figure 16: Multielectrode GCE Potentiostat. Adapted from C.N. Yarnitzky.et.al [33]

The multielectrode amperometric biosensors were designed as a CMOS time-based transducer that contains five identical working electrodes made of gold. These electrodes contain one common counter and reference electrodes. This system uses a multiplexer to choose a particular working electrode to be used at a particular time [34]. The multielectrode amperometric biosensor is shown in Figure 16.

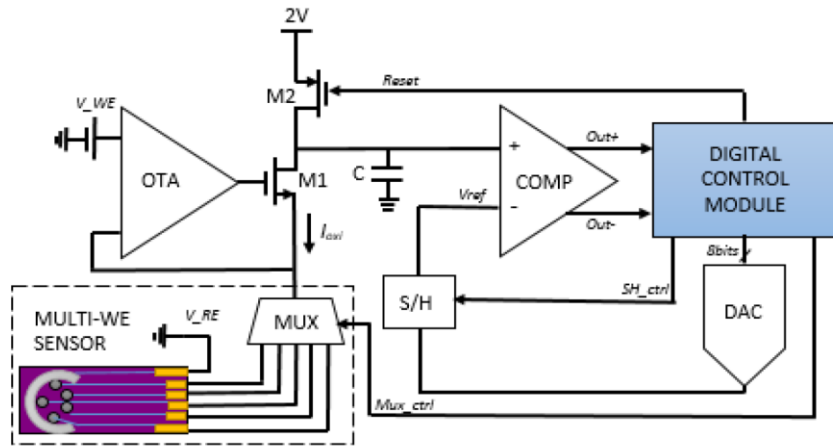


Figure 17: Multielectrode Amperometric Biosensor. Adapted from G. Massicotte.et.al [34]

In order to enable the working of multiple electrodes at the same time parallel architecture has

been proposed. This architecture was proposed wherein an array of working electrodes are connected. Multiple multiplexers are used to have one working electrode selected among the array of working electrodes. The multiplexing scheme is designed in such a way that the biasing of a particular set of electrodes do not get affected by the biasing voltages of other electrodes [35]. The parallel architecture multielectrode system is shown in Figure 18.

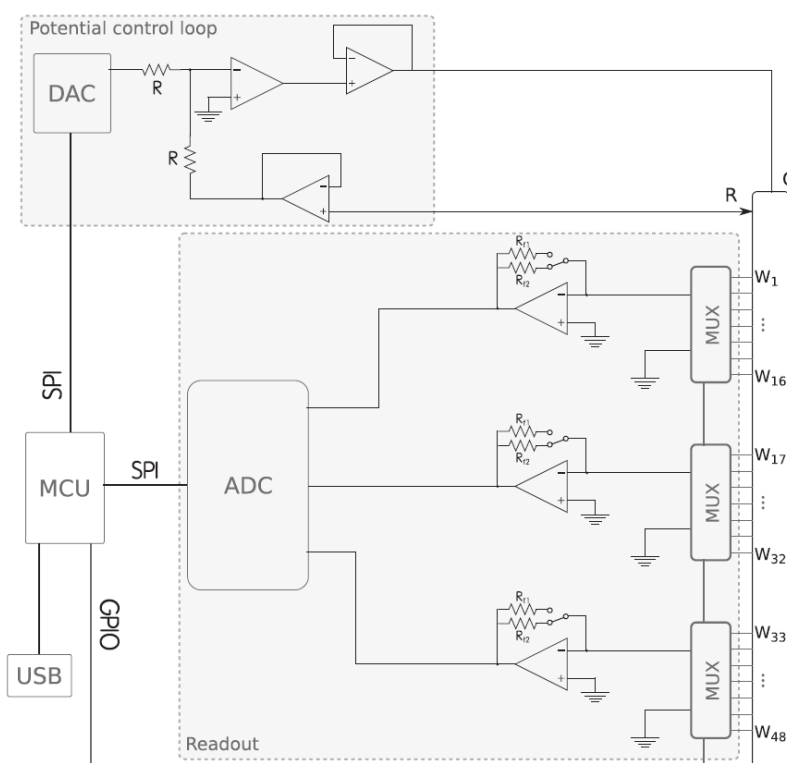


Figure 18: Parallel Architecture using Array of Working Electrodes. Adapted from I. Ramfos [35]

Commercial potentiostats are readily available and used for various electrochemical measurements. These large-sized potentiostats can be used with two, three, or four working electrodes to measure analytes simultaneously. They use a controlling software which contains control loop algorithms in order to accurately measure and correct for uncompensated

resistance. These potentiostats are not portable and cannot be integrated with mobile devices due to their large size limitation. In addition, potentiostats do not have a wireless module attached to them and attaching an external LAN facility will require the use of wire. As a result, the integration will be complicated and not very flexible. The commercial potentiostats are very high in cost and they require external AC power supply to operate them. The commercial potentiostat is shown in Figure 19 below.



Figure 19: Commercial Potentiostat. Adapted from Wikipedia.

Chapter III: Wireless Biosensor

A biosensor is an analytical device, used for the detection of a chemical substance, that combines a biological component with a physiochemical detector. Wireless Biosensors are devices that collect data from their local environment and then process and transmit the analytical information to a remote device or devices using wireless technology. There are multiple wireless biosensors that have been previously developed. The wireless biosensors use wireless techniques such as Bluetooth, Zigbee, RFID, and NFC.

Protocol	Transceiver Type	Radio Band	Data Rate	Range	Network (no. of nodes)	Features
Bluetooth	Active radio, battery powered	2.4 GHz	1 Mbps (BLE)	10–100 m	Star (8), but better peer to peer	Very high data rate, good indoor range, Smartphone compatible, good for real time data transfer
ZigBee	Active radio, battery powered	868 MHz, 915 MHz, 2.4 GHz	24 Mbps (HS) <250 kbps	10–100 m	Star/tree/mesh (65,536)	Very low-power, good indoor range, versatile network topologies, good for local sensor/actuator networks and short bursts of data
RFID	Passive transponder, batteryless or battery assisted	128–135 kHz, 13.56 MHz, 860–960 MHz	<100 kbps	<15 m, frequency dependent	Star (255), but better single transponder to reader	Ultra low-power, short range or contactless, very low data rate, smartphone compatible (13.56 MHz only), good for e-labels and small file transfers
NFC	Passive transponder, batteryless or battery assisted	13.56 MHz	<424 kbps	<5 cm	Peer to peer, single transponder to reader	Ultra low-power, contactless only, Smartphone compatible, good for secure file swaps
ISM/SRD860	Active radio, battery powered	433 MHz, 863–870 MHz	<200 kbps	50 m–2 km	Yes, dependant on specific protocol	Very low-power, good range, low data rate, good for local sensor/actuator networks
Other	Depends on the specific transceiver and protocol deployed					

Figure 20: The Comparison between various wireless standards. Adapted from H. Sillanpää et.al [36]

The Bluetooth wireless standard is the most commonly used, and NFC and RFID are the standards which are currently popular and are commonly used in Smartphones. The wireless sensor networks refer to the collection of sensors that are used to collect information and

transmit the information using wireless techniques to transmit the information onto a computer/ wireless device in order to monitor the data. Wireless sensors have been designed for monitoring the long-term physiological conditions like Diabetes, Glaucoma etc. A wireless biosensor has been proposed by Fong et al., wherein the wireless biosensor is printed on a single substrate using inkjet printing. The heart of this biosensor is a commercial NRF51822 System on Chip (SoC) from Nordic Semiconductor. The required line widths could be easily reached with inkjet printing. SoC offers the required calculation capacity, analog-to-digital converter, and radio that utilizes the Bluetooth low energy protocol. In addition, there is the antenna, balanced to unbalanced transformer balun, bio signal amplifier, electrodes, and the required discrete components. The components are attached with conductive adhesive and underfill is placed afterwards to improve the adhesion.

The biosensor is designed to operate at 300 m from the body. The spacing between the sensor and the body are created with 300 m thick plaster. The electronics are on the top side of the substrate and on the bottom side there are only two electrodes at both ends of the sensors. The contact from the electrodes to the skin is made using hydrogel [37].

The commonly used wireless sensor networks for vehicle monitoring system is the controller area network (CAN) which has been used to continually monitor the health of drivers in vehicles using a number of sensors. These sensors are placed over steering wheel, the seat of the driver, and in wearables such as smart clothing and watches. The moment something abnormal is detected by any of the sensors; that sensor's data is passed on to the onboard diagnostic device, which is then passed onto the wireless device. Thus enabling the real time monitoring of the prolonged health problems. The sensing network consists of different non-invasive sensors that require each sensor to operate independently while collecting

measurements that is forwarded to the On-board Diagnostics (OBD) for processing.

Continual health monitoring of parameters such as blood glucose and pressure do not require a continuous power source that can run on harvested power for communication. On receiving data from the biosensors, the system will commence anomaly event detection. The biosensor that picks up abnormal readings will be assigned a higher transmission priority and automatically sends an alarm to the response center. One of the main functions of the OBD is to control the state of the software-selectable CAN interface and detect anomalies based on data received from the biosensing network. Though CAN enhances the system performance, it has a very high software expenditure and there are multiple interactions between the various nodes [37]. The Network Architecture of CAN is shown in Figure 21.

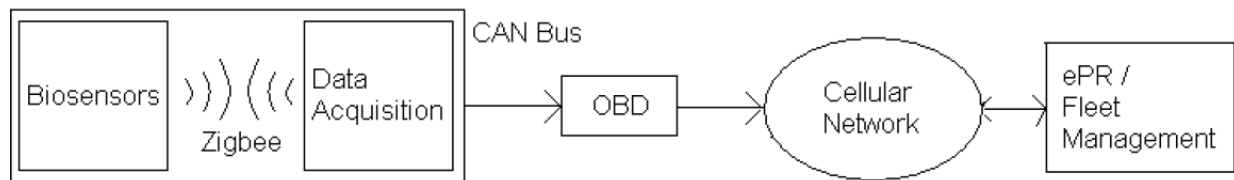


Figure 21: Network Architecture of CAN. Adapted from R. Naik. et.al [37]

Another popular wireless technology that has been implemented previously is the Ultra-Wideband Technology (UWB) that has been used for wireless sensor networks connected in an adhoc network fashion. The UWB consists of an impulse radio transceiver the transmitter uses short Gaussian derivative pulses spread over the 0-960 MHz frequency band for communication. This consumes large amounts of power and results in the longer acquisition time [38].

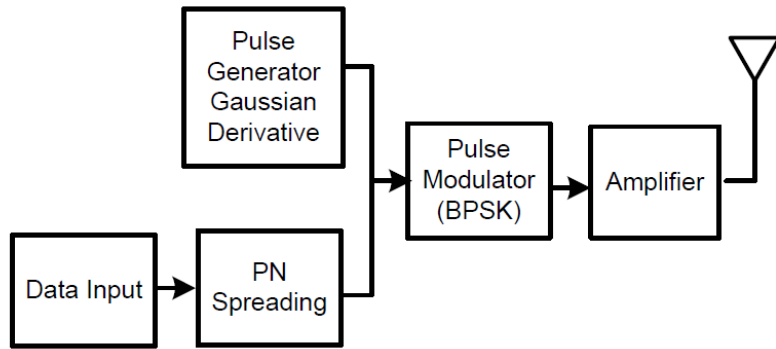


Figure 22: UWB Transmitter. Adapted from D. Albanese.et.al [38]

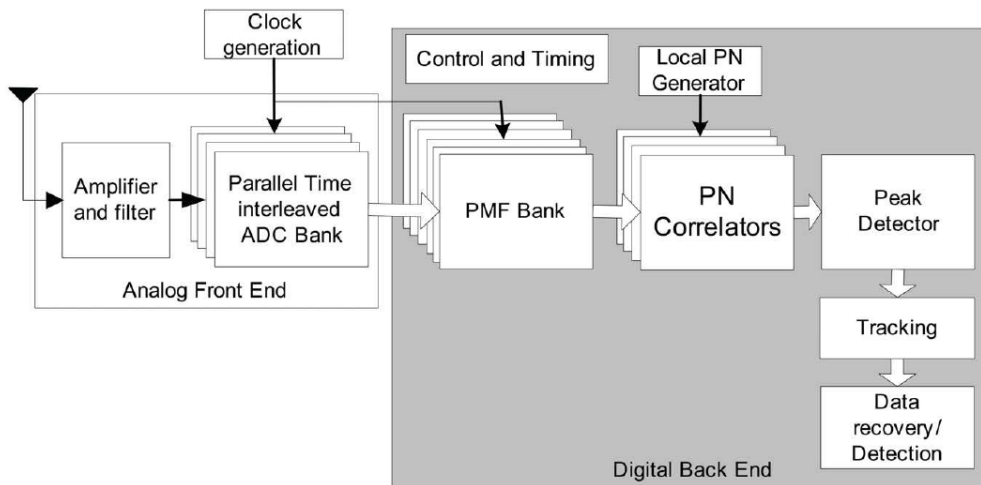


Figure 23: UWB Receiver. Adapted from D. Albanese.et.al [38]

The measuring unit in a wireless system contains - the sensible element that contains the electrochemical cell which produces electric current that is proportional to the analyte concentration which is converted to a voltage signal using the conditioning circuit. The conditioning unit contains the potentiostat which produces an output signal that is converted to voltage signal by the transducer. The Measuring Unit is as shown in Figure 24

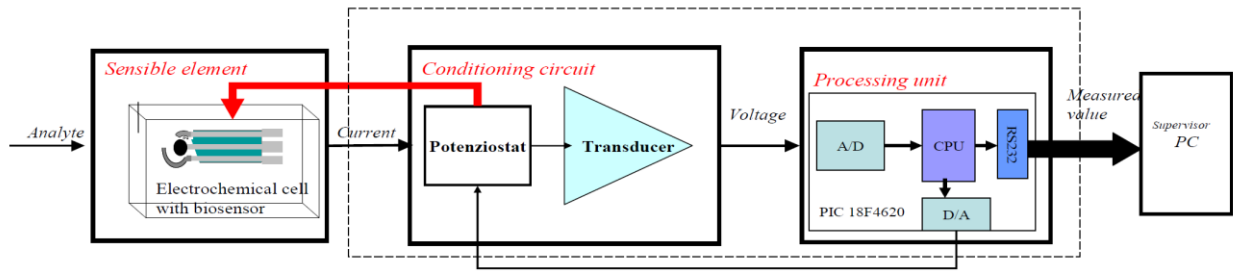


Figure 24: Measuring System. Adapted from D. Albanese.et.al [39]

The processing unit converts the incoming signal from the potentiostat circuit to the digital form, which is then displayed on the personal computer. Using all the blocks of the processing unit, the transmission of data to the PC takes time and this creates some delay. All the hardware increases the circuit complexity as well. Furthermore, an LCD is interfaced with the PC, which display the concentration values directly. Integrating the PC with the mobile device requires a wireless module to transmit the data and to synch the data up with the PC.

A. ESP8266

The first part of the Wi-Fi modules is ESP8266, a self-contained SOC with an integrated TCP/IP protocol stack that can give any microcontroller access to a Wi-Fi network. The ESP8266 is capable of either hosting an application or offloading all Wi-Fi networking functions from another application processor. Each ESP8266 module comes pre-programmed with an AT command set firmware to enable easy integration with Arduino device. The ESP8266 module is an extremely cost-effective board with a huge, and ever growing community. This module has powerful on-board processing and storage capability which allows it to be integrated with the sensors and other application specific devices through its

GPIOs with minimal development up-front and loading during runtime. Its high degree of on-chip integration allows for minimal external circuitry including the front-end module. It is designed to occupy minimal PCB area [40]. The ESP8266 module is shown in Figure 25 below.

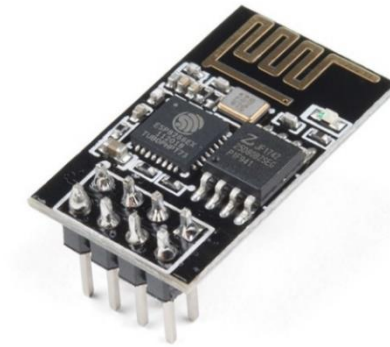


Figure 25: ESP8266. Adapted from Sparkfun.com [40]

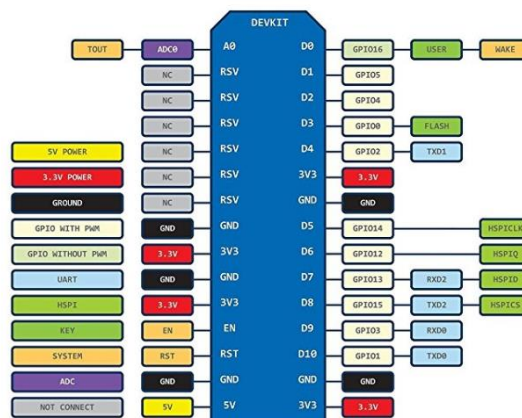
The ESP-12 E module allows for access to many features of the ESP8266 via the 11 GPIO pins and one analog-to-digital converter (ADC) with a 10-bit resolution and 8 Mbit flash embedded. Esp-12E Esp8266 Wi-Fi module is a low power consuming model of the already ultra-low consuming UART-Wi-Fi module designed especially for mobile devices and IoT applications. The physical devices can be connected to a Wi-Fi wireless network, internet, or intranet communication and networking systems. The module supports standard IEEE802.11 b/g/n agreement and complete TCP/IP protocol stack. These capabilities enable multiple modules to be added to the existing device network or use as a standalone device to build a separate network controller [41].

NodeMcu is an open source IoT platform. This includes the firmware which runs on the ESP8266 Wi-Fi SoC and hardware, which is based on the ESP-12 module. The NodeMCU

module is shown in Figure 26 below. The pinout of NodeMCU [42] is as shown in Figure 27.



Figure 26: NodeMCU. Adapted from Wikipedia.



Since, we need to measure two current values at the same time and transmit, two NodeMcu boards have been used in order to simultaneously transmit two concentration values. The Arduino module has eight analog pins, but it is big in size and it does not have LAN facility with wireless connection. Though we have used two NodeMcu boards, it is smaller in size and hence the circuit size is compact. An LED is used to connect between the pin D4 and ground to indicate if the concentration values of glucose and hydrogen peroxide decreases below a certain level of concentration. Software implementation is done using Arduino IDE. The open-source Arduino Software (IDE) makes it easy to write code and upload it to the board. It runs on Windows, Mac OS X, and Linux. The environment is written in Java and based on Processing and other open-source software.

The Adafruit IO is used to display the real-time data online. This is a free cloud service which helps to manage the data in real-time. The current value that is measured between the counter electrode and the working electrode is fed to the analog pin and this is used to calculate the concentration values for both the glucose as well as the hydrogen peroxide solutions. These real-time concentration values are displayed on the Adafruit dashboard. This dashboard can be used to display 30 data points per minute and the storage can hold up to 30 days of data. The dashboard contains the feeds, which are at the core of the Adafruit IO. They hold the data that has been uploaded and the meta-data about the data that the sensors push to Adafruit IO. The real-time data that is transmitted on to the Adafruit website is protected as each user is given a unique code to access the data. The data is secure, and it is time-tracked. On an Arduino, there are two different libraries that can be used to access the Adafruit IO. One library is based on the REST API and the other library is based on the MQ Telemetry Transport (MQTT) API. The difference between these libraries is that MQTT keeps a connection to the service open so

it can quickly respond to feed changes. The REST API only connects to the service when a request is made so it is a more appropriate choice for projects that sleep for a period of time (to reduce power usage) and wake up only to send/receive data is desired. In this work we implemented the MQTT library in order to track the real-time data.

The MQTT plays an important role in IoT devices to send or publish information about a given topic to a server that functions as a message broker. The MQTT library is used in the Arduino IDE code and the analog input is monitored and received by the analog pin A0. This data is used in further calculations. The MQTT library helps to send the calculated data onto the Adafruit dashboard where the data is published under the feeds created by the user [43].

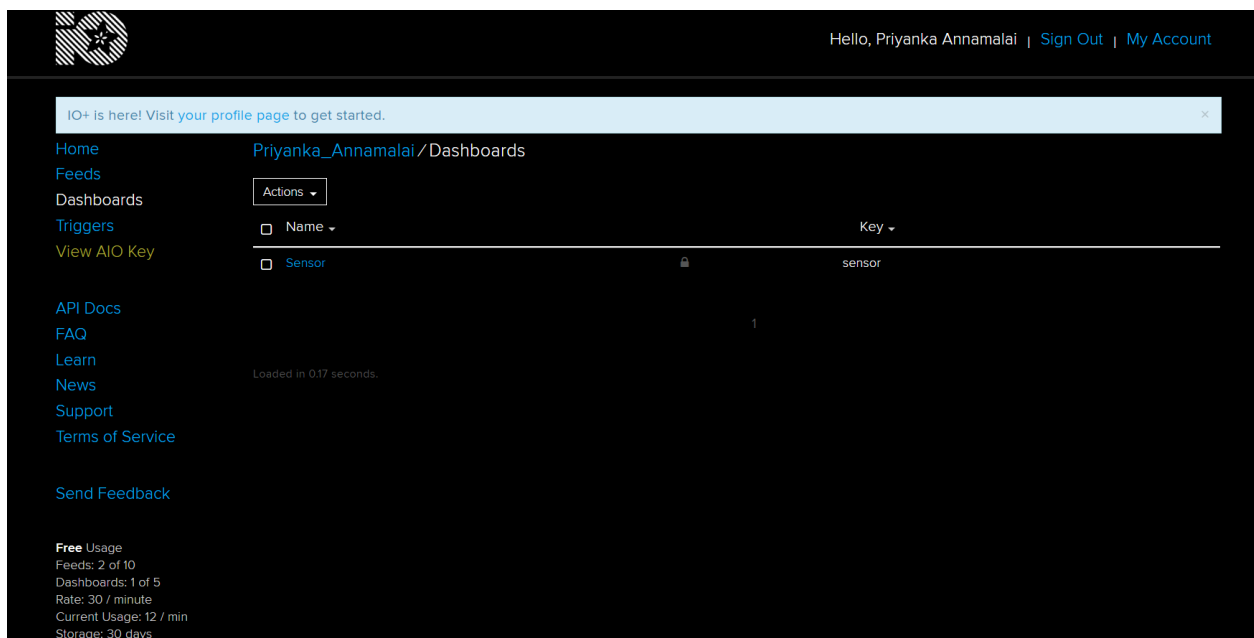
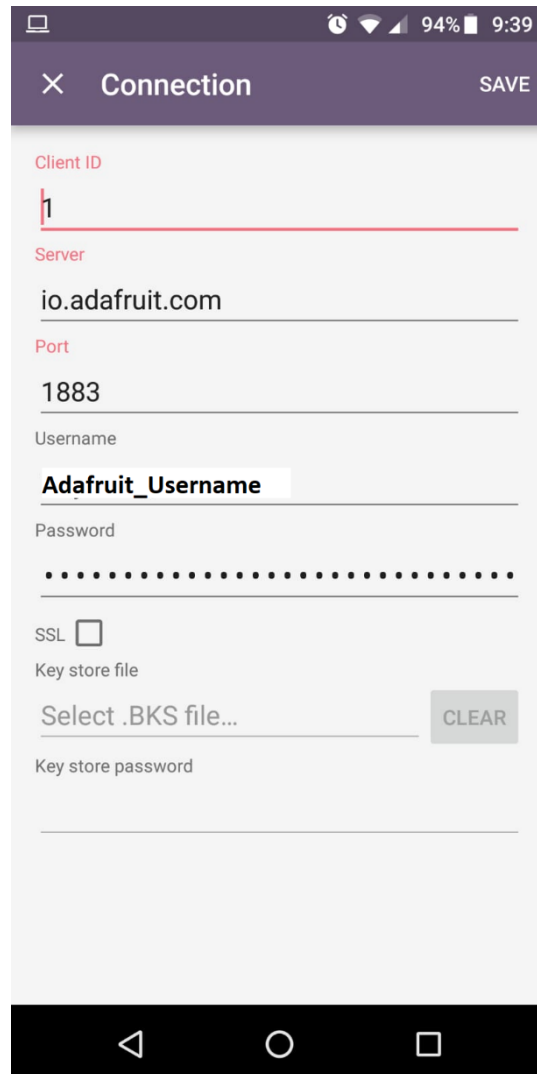


Figure 28: Adafruit Website

The Adafruit Dashboard is as shown in Figure 28. Sensor is a dashboard feed name where the real-time data of the sensor is displayed. MQTT IoT is an android application which enables the user to enter the feed name that requires monitoring and displaying of real-time data. This

helps to take required actions when the concentration levels of glucose and hydrogen peroxide solutions go below the desired levels. The MQTT application displaying the concentration values of glucose is shown in Figure 29.



The screenshot shows a mobile application interface for MQTT connection. At the top, there is a status bar with icons for a laptop, a clock, a Wi-Fi signal, a cellular signal, 94% battery, and the time 9:39. Below the status bar is a purple header bar with a close icon (X), the title "Connection", and a "SAVE" button. The main form area has a light gray background and contains the following fields: "Client ID" with the value "1", "Server" with the value "io.adafruit.com", "Port" with the value "1883", "Username" with the value "Adafruit_Username", and "Password" which is masked with dots. There is an "SSL" checkbox which is unchecked. Below the SSL checkbox is a "Key store file" section with a "Select .BKS file..." button and a "CLEAR" button. At the bottom of the form is a "Key store password" field. The entire form is enclosed in a white border. At the very bottom of the screen is a black Android navigation bar with the back, home, and recent apps icons.

Figure 29: MQTT Mobile Application

Chapter IV: Construction of wireless bipotentiostat circuit for analyte interrogation

The enzyme-based finger-pricking method is the most commonly used diabetic assessment. However, the procedure is invasive, inconvenient, requires patient compliance, and may cause infection during the blood sampling processes [26]. An alternative method uses near-infrared spectroscopy and provides a noninvasive way to monitor the glucose levels in the body. This method analyzes the light reflection or transmission spectrum in the fingertip to infer metabolic concentration [26]. Due to challenges of interference with other biochemicals, poor signal strength, and calibration issues this method is not sufficiently accurate for clinical use [26]. Therefore, ongoing research focuses on the development of miniaturized noninvasive and continuous biosensing systems. H_2O_2 is reactive oxygen species which can respond to various cellular targets' functions as a signaling molecule that controls different essential processes in mammals and plants. Excessive H_2O_2 can cause serious diseases like cancer, stroke etc. Hence, real-time monitoring of Glucose and H_2O_2 play an important role in the diagnosis of diseases and treatment of diseases. There is a need for a device which can measure the levels of glucose and Hydrogen peroxide in the body and this device should be small so that it can be portable and easier to construct. A small Bipotentiostat is designed to measure the two solutions simultaneously in the human body.

Here the constructed bipotentiostat block is comprised of two working electrodes: a common counter and a reference electrode. The bipotentiostat is designed using LM 358 operational amplifiers (op-amps) and IC UM 741 logic inverters. A voltage of 5 V is applied

to the first op-amp and a voltage of 1.4 V is applied to the op-amp U4, which results in a voltage reference of 3.6 V across the working and reference electrodes. The resulting current flow from the counter electrode to the working electrode 1 is fed to a logic inverter U5 whose output is fed to the working electrode 2 (Figure 30). Chronoamperometry is performed using the constructed bipotentiostat connected to the two working electrodes in the presence of a phosphate buffer as well as glucose, and hydrogen peroxide (H_2O_2) solutions. The glucose solution current output ranges in terms of microamperes while the H_2O_2 current output ranges in terms of milliamperes.

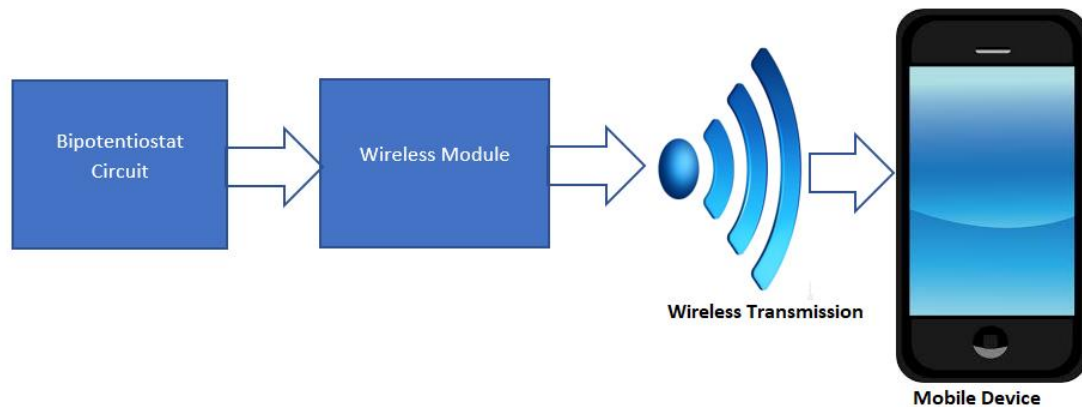


Figure 30: Wireless Bipotentiostat Block Diagram

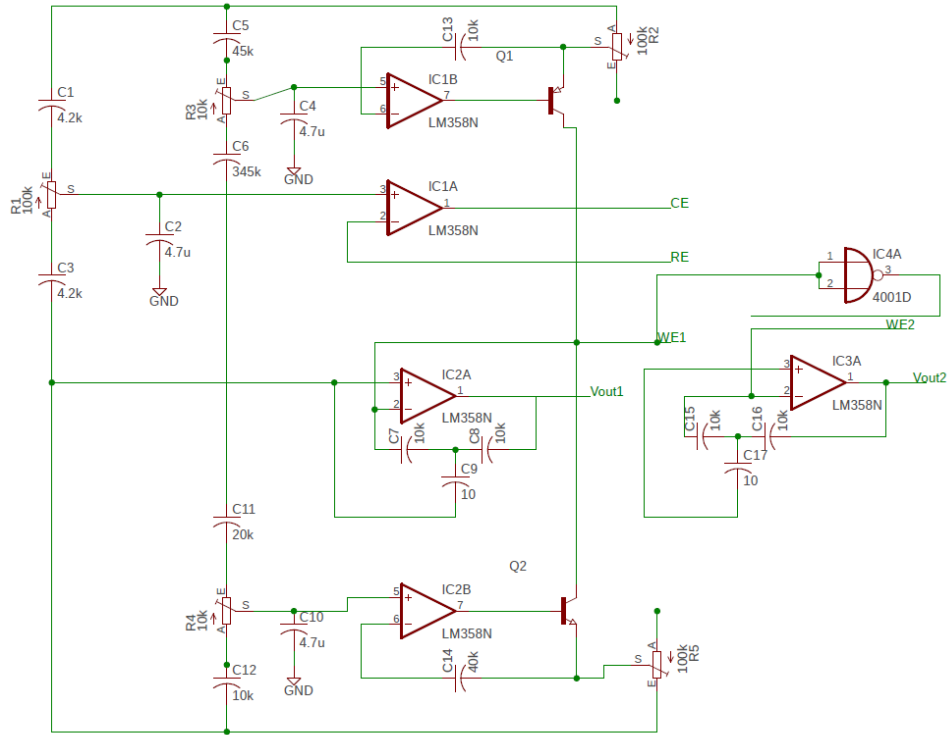


Figure 31: Schematic of Bipotentiostat

The Wireless block consists of the ESP8266 Nodemcu-12 wireless module equipped with a microcontroller that processes the data. Using TCP/IP protocols and the Arduino IDE, data is transmitted wirelessly to the Adafruit webserver. A 100 k Ω resistor is connected across the counter electrode (CE) and working electrode (WE). The output current from the bipotentiostat is fed into the analog pin, A0 of the ESP8266. The ground and voltage inputs are connected to ground and V_{DD} , respectively. These analog values are sampled every 3 ms and the output current is transmitted to the Adafruit webserver. The Adafruit cloud service (Adafruit IO) is used to display the concentration values obtained from the bipotentiostat by monitoring the output current from the electrodes in real-time. A dashboard is created on the webserver to display the data and synched with a mobile device via the Adafruit IO. Thereby, enabling the

data to be monitored on a mobile device using the MQTT dashboard application.

A. Materials

Glucose solution, mercaptopropionic acid (MPA), hydrogen peroxide, horseradish peroxidase (HRP), $\text{HAuCl}_4 \cdot n\text{H}_2\text{O}$, ascorbic acid (AA), uric acid (UA), N-(3-Dimethylaminopropyl)-N'-ethylcarbodiimide hydro-chloride (EDC), and N-Hydroxysuccinimide (NHS) were required from Sigma Aldrich. PBS buffer (PBS) pH 7.4 was prepared with 18.2 M Ω cm Milli-Q water. Chronoamperometry measurements were performed using the fabricated bipotentiostat and HP Agilent E3630A Triple Output DC Power Supply.

B. Electrode Construction

The 20 mm long and 0.2 mm thick tungsten and gold wires were cleaned with IPA, ethanol, and dried with N_2 gas to serve as the working electrodes. The first working electrode comprised of gold functionalized with colloidal platinum electrodeposited from platinizing solution at an applied potential of -225 mV (Ag/AgCl) for 1500 s, using chronoamperometry. Loosely bound platinum particles are removed from the wire surface by dipping the electrodeposited electrode in DI water. The dried electrode is then coated with 1% chitosan. The second working electrode was comprised of tungsten wire modified with gold nanoparticles (AuNPs) that is electrodeposited from 1 mM $\text{HAuCl}_4 \cdot n\text{H}_2\text{O}$ solution at -0.2 V (Ag/AgCl) for 50 s followed by incubation in 1 mM mercaptopropionic acid (MPA) in PBS for 1 hour to form a self-assembled monolayer with carboxylic acid head group on the surface of the AuNPs. The carboxylic acid head group of MPA was then activated by 0.8 mg EDC and 2.2 mg NHS along with 1 mg of HRP in 100 mM PBS 7.4 overnight at -20 °C. In presence of the EDC, the N-hydroxyl group of the NHS interacts with the carboxyl groups to form reactive sites, where the amino group of

HRP displaces the succinimide group of NHS to form covalent bonding. The modified region of the tungsten wire exhibited a surface area of 6.345 mm². The electrodes are then inserted into the electrolyte for further electrochemical detections using the constructed bipotentiostat.

Chapter V: Experimental Results

In this study, the bipotentiostat was used to perform chronoamperometry using the gold-platinized and AuNPs-HRP electrodes for simultaneous glucose and H_2O_2 detection, respectively. The output current is measured for various concentrations of glucose and H_2O_2 . Upon spiking the 100 mM phosphate buffer with glucose, an increase was observed in the output current of working electrode 1 as the result of the oxidation of glucose by the gold colloidal-Pt composite. As the glucose concentration is increased, increasing output currents were observed indicating that the bipotentiostat operating in amperometry mode is able to differentiate various concentrations of glucose. The corresponding calibration curve is depicted in Figure 32. A linear dynamic range of 1 mM to 20 mM is observed. The glucose sensor exhibited a sensitivity of $0.139 \text{ mA /mM-cm}^2$ much lower than those reported by Slaughter et al. and Liao et al. [12, 27].

Similarly, in the presence of H_2O_2 , the output reduction current increased with increasing H_2O_2 concentrations as expected at working electrode 2 (Figure 33). This indicates that the bipotentiostat can differentiate various levels of H_2O_2 concentrations as the result of the reduction of H_2O_2 at the AuNPs-HRP electrode. A linear dynamic range of 1 - 6 μM and 11 - 20 μM was observed with a sensitivity of $0.021 \text{ mA /mM cm}^2$ (Figure 33), which is higher in sensitivity than 4.86 A/ M cm^2 [11]. This demonstrates that the constructed system is capable of detecting both glucose and H_2O_2 concentration levels quantitatively.

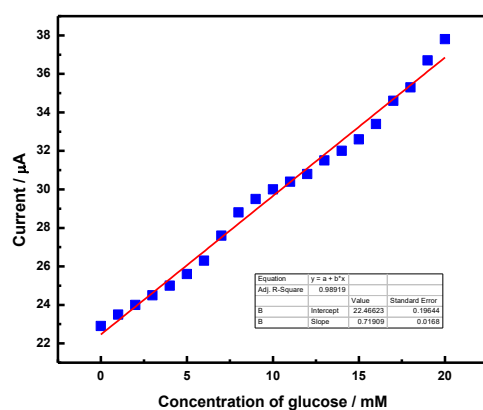


Figure 32: Glucose calibration plot measured using constructed bipotentiostat (100 mM PBS, pH 7.4).

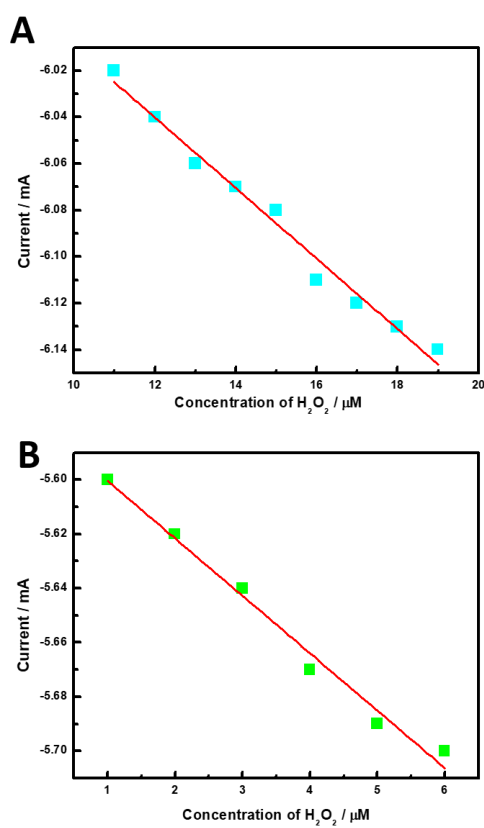


Figure 33: H_2O_2 calibration plot measured using constructed bipotentiostat (100 mM PBS, pH 7.4).

The response of the bipotentiostat system in the presence of competing and non-competing

analytes are examined to evaluate the selectivity of sensors. Uric acid (UA) and ascorbic acid (AA) are used to perform the selectivity evaluation. Ideally in the presence of interference species the sensors will not show any change in current response to UA and AA as the glucose and H_2O_2 sensors should be selective towards glucose and H_2O_2 , respectively. Figure 34 shows the current response of the glucose sensor in the presence of glucose, UA and AA. Upon the addition of 1 mM glucose the output oxidation current increased and remained stable. When 1 mM of ascorbic acid and uric acid were introduced to the sensor at different time point, no change was observed in the oxidation current output. Furthermore, after the addition of 2 mM glucose, the output oxidation current response immediately increased indicating that the system selective towards glucose and not UA and AA.

The selectivity profile of the H_2O_2 sensor is depicted in Figure 35, wherein the addition of 1 μM H_2O_2 results in an increase in the reduction current response. As expected, there was no change in the current response upon the addition of 1 μM of AA and UA. An additional aliquot of 1 μM of hydrogen peroxide was added and an increase was observed in the reduction current indicating that the H_2O_2 sensor was selective towards H_2O_2 and not UA and AA.

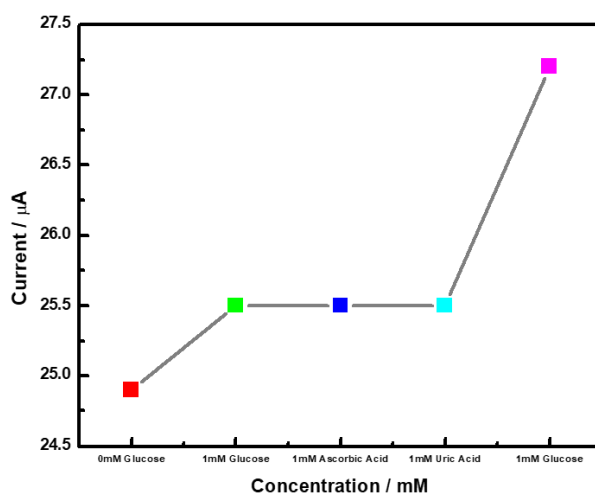


Figure 34: Selectivity behavior of the glucose sensor measured in the presence of interference species.

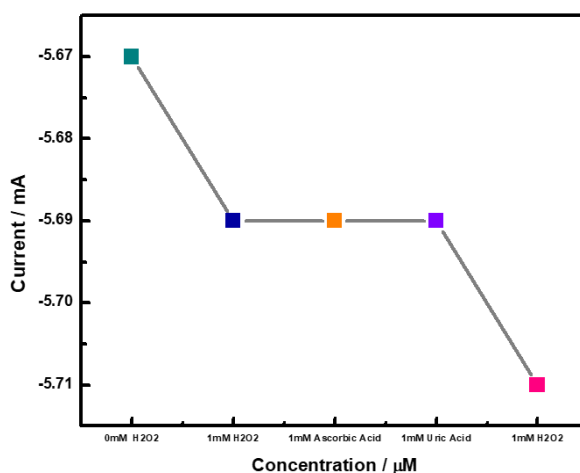


Figure 35: Selectivity behavior of the H_2O_2 sensor measured in the presence of interference species.

Using Adafruit IO, the dashboard created on the webserver was used to display the data and synced with a mobile device enabling the tracking of the concentration measurements using current values. Based on the calibration curves, it was observed that the concentration of glucose is directly correlated to the output oxidation current measured. As the glucose concentration increases, the output current value also increases. Hence, the slope of the calibration curve is positive. Since the slope “m” (sensitivity) is the change in y-values (current) divided by the change in x-values (concentration), the concentration of the analyte can be calculated in real-time. The y-intercept in the equation indicated by “c,” is assigned the first current value sensed by the analog pin in the absence of the analyte of interest. For the H_2O_2 sensor, when the concentration increases, the reduction current increases, wherein the slope is negative. The calculated concentration values are then displayed on the dashboard using the linear relationship generated from the calibration curve.

The constructed bipotentiostat circuit, designed using operational amplifiers and logic inverter,

enabled the measurement of two analytes, glucose and H_2O_2 , at the same time. The overall cost of the bipotentiostat is less than \$50. The small form factor of the device makes it portable and a good alternative for point-of-use testing. Additionally, the system is integrated with the wireless module to enable real-time data monitoring via a mobile device. The device is integrated with an LED to indicate when the levels of glucose and hydrogen peroxide have gone below a pre-determined value. The experimental setup is shown in Figure 36 below.

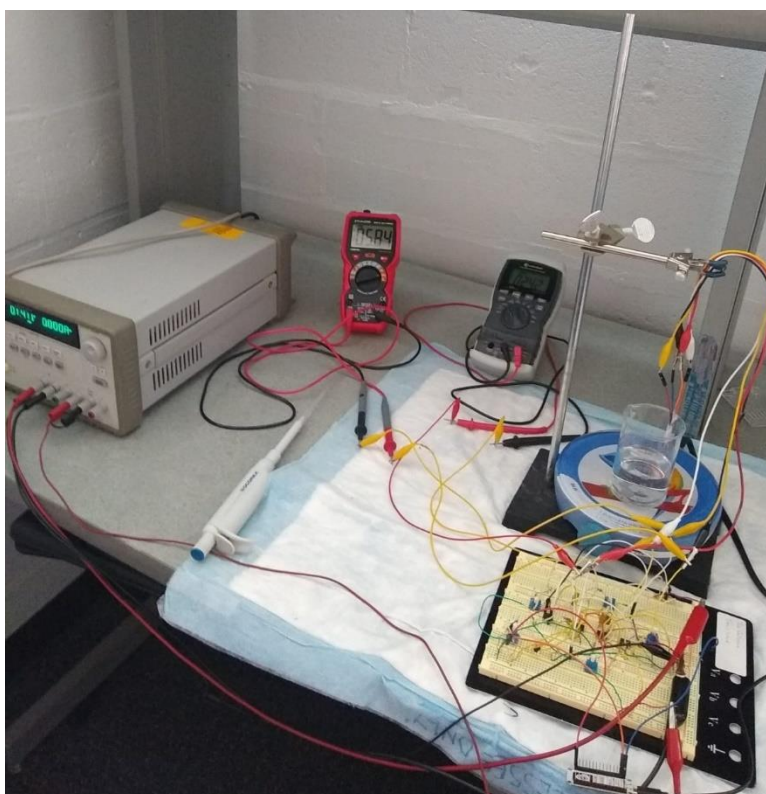


Figure 36: Experimental Setup

The concentration values are calculated using the linear curve equation. The concentration and current values are directly proportional to each other according to the formula given below:

$$i = \frac{nFA\sqrt{D}C_{ox}}{\sqrt{(\pi t)}}$$

where n is the number of electrons transferred per electroactive molecule or ion, F is the Faraday constant, A is the area of the electrode surface in cm^2 , D is the diffusion coefficient in cm^2/s , C_{ox} is the concentration of the oxidized species in mol/cm^3 , and t is the time in seconds. Most of the terms in the above equation are constants for a particular analyte and hence the current and the concentration values can be calculated using the linear slope equation $y = mx + c$, where y represents the concentration values and the x represents the current values. The c value is the same as the current values at 0 mM concentration and the m value is approximately equal to the slope calculated on the plot for current vs concentration values previously. This value needs to be adjusted using the trial and error method. The slope value is approximately equal to the previous slope values.

The Adafruit website dashboard displaying the concentrations of glucose is as shown in the Figure 37.

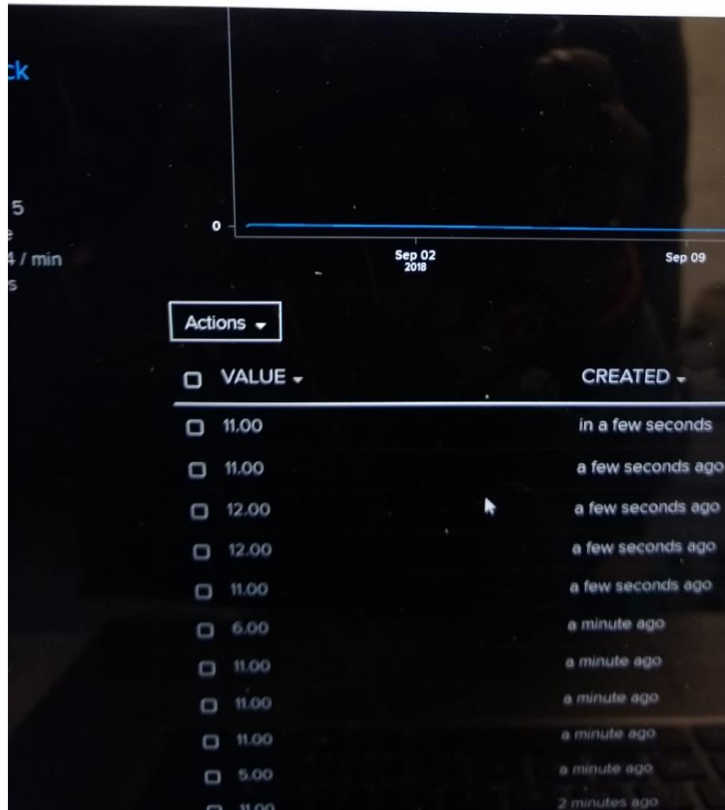


Figure 37: Adafruit website displaying the concentration of glucose

The MQTT mobile application will be in sync with the Adafruit IO and the current concentration value can be tracked as shown in Figure 38 below.

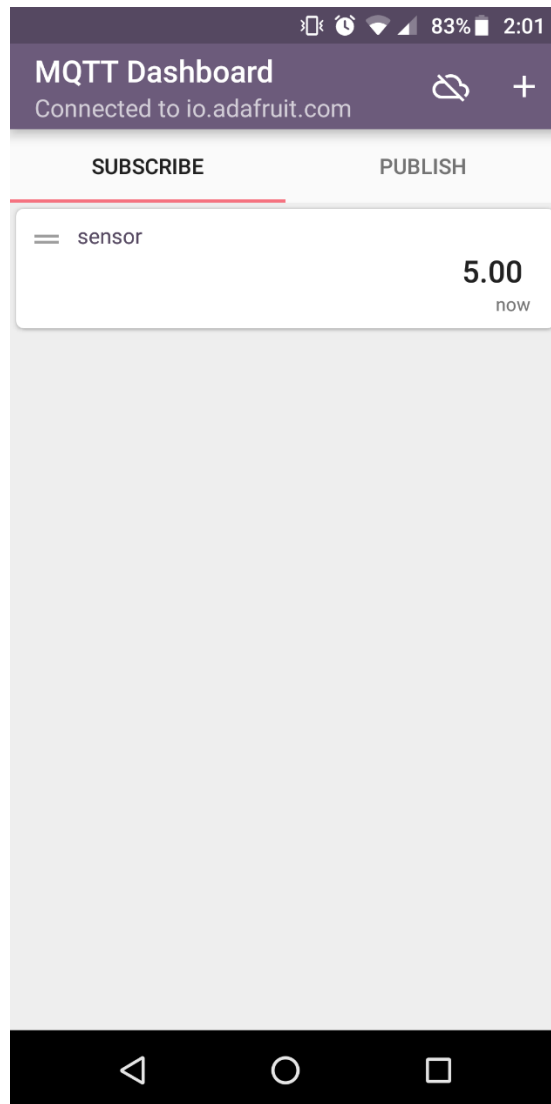


Figure 38: MQTT Application showing glucose concentration

Chapter VI: Conclusion

In this study, we demonstrated the construction of a bipotentiostat system. When coupled with glucose and H_2O_2 sensors, it is capable of detecting and distinguishing between the various concentration levels of glucose and H_2O_2 with a fine degree of sensitivity and selectivity. The bipotentiostat system utilized the ESP8266 device to enable wireless data transmission and processing of the sensed oxidation and reduction output currents in a more affordable manner. The bipotentiostat and sensors provided an approach to developing cost-effective point-of-use biosensor devices. This platform can detect glucose and H_2O_2 rapidly and inexpensively while serving as a detection tool in areas with limited access to expensive technology.

A. Future Work

The future work involves making the circuit smaller in size. The Bipotentiostat measures current values in the range of $20\ \mu\text{A} - 7\ \text{mA}$, the range of current values can be further expanded by measuring current values in terms of nanoamperes. Thus, the sensitivity of the device can be improved. Also, machine learning techniques like Support Vector Machine (SVM), perceptron etc. can be used, and the model will be trained to learn the behaviour of current against the concentration values. This will make the model dynamic instead of static implementation.

References

- [1] Shi, Yuankai, and Frank B. Hu. "The global implications of diabetes and cancer." *The lancet* 383.9933 (2014): 1947-1948.
- [2] *Estimates Of Diabetes And Its Burden In The United States*. National Diabetes Statistics Report, 2017, <http://www.diabetes.org/assets/pdfs/basics/cdc-statistics-report-2017.pdf>. Accessed 15 Dec 2018.
- [3] Miller, Evan W., Bryan C. Dickinson, and Christopher J. Chang. "Aquaporin-3 mediates hydrogen peroxide uptake to regulate downstream intracellular signaling." *Proceedings of the National Academy of Sciences* 107.36 (2010): 15681-15686.
- [4] Dryden, Michael DM, et al. "Upon the shoulders of giants: open-source hardware and software in analytical chemistry." *Analytical chemistry* 89.8 (2017): 4330-4338.
- [5] Giordano, Gabriela F., et al. "Point-of-use electroanalytical platform based on homemade potentiostat and smartphone for multivariate data processing." *Electrochimica Acta* 219 (2016): 170-177.
- [6] Sun, Alexander C., et al. "An efficient power harvesting mobile phone-based electrochemical biosensor for point-of-care health monitoring." *Sensors and Actuators B: Chemical* 235 (2016): 126-135.

[7] Gao, Wei, et al. "Fully integrated wearable sensor arrays for multiplexed in situ perspiration analysis." *Nature* 529.7587 (2016): 509.

[8] Imani, Somayeh, et al. "A wearable chemical–electrophysiological hybrid biosensing system for real-time health and fitness monitoring." *Nature communications* 7 (2016): 11650.

[9] Number of mobile phone users worldwide 2015-2020 | Statista
<https://www.statista.com/statistics/274774/forecast-ofmobile-phone-users-worldwide/>

[10] Dai, Hongxia, et al. "A novel biosensor based on boronic acid functionalized metal-organic frameworks for the determination of hydrogen peroxide released from living cells." *Biosensors and Bioelectronics* 95 (2017): 131-137.

[11] Salimi, Abdollah, et al. "Nanomolar detection of hydrogen peroxide on glassy carbon electrode modified with electrodeposited cobalt oxide nanoparticles." *Analytica chimica acta* 594.1 (2007): 24-31.

[12] Slaughter, Gymama and Joshua Sunday. "Fabrication of enzymatic glucose hydrogel biosensor based on hydrothermally grown ZnO nanoclusters." *IEEE Sensors Journal* 14.5 (2014): 1573-1576.

[13] Xu, Bin, et al. "A highly sensitive hydrogen peroxide amperometric sensor based on MnO₂-modified vertically aligned multiwalled carbon nanotubes." *Analytica chimica*

acta674.1 (2010): 20-26.

[14] Bai, Yu-Hui, et al. "Choline biosensors based on a bi-electrocatalytic property of MnO₂ nanoparticles modified electrodes to H₂O₂." *Electrochemistry Communications* 9.10 (2007): 2611-2616.

[15] Baingane, Ankit and Gymama Slaughter. "Self-powered electrochemical lactate biosensing." *Energies* 10.10 (2017): 1582.

[16] Hasan, Md Qumrul, et al. "Fabrication of highly effective hybrid biofuel cell based on integral colloidal platinum and bilirubin oxidase on gold support." *Scientific reports* 8.1 (2018): 16351.

[17] Wang, Xue, et al. "Synthesis of CuO nanostructures and their application for nonenzymatic glucose sensing." *Sensors and Actuators B: Chemical* 144.1 (2010): 220-225.

[18] Ping, Jianfeng, et al. "Copper oxide nanoparticles and ionic liquid modified carbon electrode for the non-enzymatic electrochemical sensing of hydrogen peroxide." *Microchimica Acta* 171.1-2 (2010): 117-123.

[19] Li, Yali, et al. "Gold nanoparticles mediate the assembly of manganese dioxide nanoparticles for H₂O₂ amperometric sensing." *Electrochimica Acta* 55.18 (2010): 5123-5128.

[20] Slaughter, Gymama E., et al. "Improving neuron-to-electrode surface attachment via alkanethiol self-assembly: an alternating current impedance study." *Langmuir* 20.17 (2004): 7189-7200.

[21] Narayanan, Jeyaraman S., and Gymama Slaughter. "AuNPs-HRP microneedle biosensor for ultrasensitive detection of hydrogen peroxide for organ preservation." *Medical Devices & Sensors* 1.2 (2018): e10015.

[22] Wang, Zonghua, et al. "DNA assembled gold nanoparticles polymeric network blocks modular highly sensitive electrochemical biosensors for protein kinase activity analysis and inhibition." *Analytical chemistry* 86.12 (2014): 6153-6159.

[23] Liu, Lin, et al. "Highly sensitive and label-free electrochemical detection of microRNAs based on triple signal amplification of multifunctional gold nanoparticles, enzymes and redox-cycling reaction." *Biosensors and Bioelectronics* 53 (2014): 399-405.

[24] Afkhami, Abbas, et al. "Surface decoration of multi-walled carbon nanotubes modified carbon paste electrode with gold nanoparticles for electro-oxidation and sensitive determination of nitrite." *Biosensors and Bioelectronics* 51 (2014): 379-385.

[25] Wearable Sweat Sensor Pioneer Issued Key Device Patent

<https://www.businesswire.com/news/home/20181218005089/en/Wearable-Sweat-Sensor> Pioneer-

[26] Bruen, Danielle, et al. "Glucose sensing for diabetes monitoring: recent developments." *Sensors* 17.8 (2017): 1866.

[27] Liao, Yu-Te, et al. "A $3\text{-}\mu\text{m}$ CMOS Glucose Sensor for Wireless Contact-Lens Tear Glucose Monitoring." *IEEE Journal of Solid-State Circuits* 47.1 (2012): 335-344.

[28] **Kamat**, Prashant. *Potentiostat*. Prashant Kamat, 2019, <https://www3.nd.edu/~kamatlab/documents/facilities/potentiostat.pdf>. Accessed 10 Feb 2019.

[29] Potentiostat/Galvanostat Electrochemical Instrument Basics
<https://www.gamry.com/application-notes/instrumentation/potentiostat-fundamentals/>

[30] **Gabor**, Galbacs. *Electroanalytical Methods*. 2010, <http://www2.sci.u-szeged.hu/inorg/Physical%20analysis%202010%20-%20Electroanalytical%20methods.pdf>. Accessed 10 Feb 2019.

[31] Electroanalytical methods
https://en.wikipedia.org/wiki/Electroanalytical_methods

[32] Huang, Yue, and Andrew J. Mason. "A redox-enzyme-based electrochemical biosensor with a CMOS integrated bipotentiostat." *2009 IEEE Biomedical Circuits and Systems Conference*. IEEE, 2009.

- [33] Yarnitzky, Chaim N. "Part I. Design and construction of a potentiostat for a chemical metal-walled reactor." *Journal of Electroanalytical Chemistry* 491.1-2 (2000): 160-165.
- [34] Massicotte, Genevive, et al. "Multi-electrode amperometric biosensor for neurotransmitters detection." *2013 IEEE Biomedical Circuits and Systems Conference (BioCAS)*. IEEE, 2013.
- [35] Ramfos, Ioannis, et al. "A compact hybrid-multiplexed potentiostat for real-time electrochemical biosensing applications." *Biosensors and Bioelectronics* 47 (2013): 482-489.
- [36] Sillanpää, Hannu, et al. "Inkjet printed wireless biosensors on stretchable substrate." *2014 International Conference on Electronics Packaging (ICEP)*. IEEE, 2014.
- [37] Fong, Alvis Cheuk M., et al. "Wireless biosensing network for drivers' health monitoring." *2016 IEEE International Conference on Consumer Electronics (ICCE)*. IEEE, 2016.
- [38] Naik, Rohit, Jugdutt Singh, and H. P. Le. "Intelligent Communication Module for Wireless Biosensor Networks." *Biosensors*. IntechOpen, 2010.
- [39] Albanese, Donatella, et al. "Biosensor-based intelligent measurement system for wine fermentation monitoring." *2010 43rd Hawaii International Conference on System Sciences*.

IEEE, 2010.

[40] WiFi Module - ESP8266 - WRL-13678 - SparkFun Electronics
<https://www.sparkfun.com/products/13678>

[41] Esp-12E Esp8266 Wifi Module: rhydoLABZ INDIA
<https://www.rhydolabz.com/wireless-wifi-c-130134/esp12e-esp8266-wifi-module-p-2503.htm>

[42] NodeMCU
<https://en.wikipedia.org/wiki/NodeMCU>

[43] Adafruit IO
<https://io.adafruit.com>

[44] Wilson, George S., et al. "Implantable glucose sensor." U.S. Patent No. 5,165,407. 24 Nov. 1992.

